Available online at www.sciencedirect.com
ScienceDirect
Journal of Power Sources 173 (2007) 166–171
JOURNAL OF POWER SOURCES
www.elsevier.com/locate/jpowsour

Short communication

Dimethoxymethane and trimethoxymethane as alternative fuels for fuel cells

Raghuram Chetty [a,b,*], Keith Scott [b]

[a] *Laboratory of Industrial Chemistry, Ruhr University Bochum, Germany*
[b] *School of Chemical Engineering & Advanced Materials, Newcastle University, United Kingdom*

Received 2 June 2007; received in revised form 21 July 2007; accepted 29 July 2007
Available online 7 August 2007

Abstract

The electrooxidation of dimethoxymethane (DMM) and trimethoxymethane (TMM) was studied at different platinum-based electrocatalysts deposited onto a titanium mesh substrate by thermal decomposition of chloride precursors. Half-cell tests showed an increase in oxidation current for the methoxy fuels at the platinum electrode with the alloying of ruthenium and tin. Increase in reaction temperature and reactant concentration showed an increase in current density for the mesh-based anodes similar to carbon-supported catalysts. Single fuel cell tests, employing the titanium mesh anode with PtRu and PtSn catalysts showed maximum power densities up to 31 mW cm^{-2} and 48 mW cm^{-2} for 1.0 mol dm^{-3} aqueous solutions of DMM and TMM, respectively at 60 °C using oxygen.

Keywords: Dimethoxymethane; Trimethoxymethane; Oxidation; Electrocatalyst; Titanium mesh; Fuel cells

1. Introduction

Direct liquid fuel cells based on methanol have been demonstrated to have good performance characteristics and are already of commercial interest [1–4]. In order to extend the practical application of low-temperature fuel cells and facilitate their penetration into the transport market it is desirable to increase the number of liquid fuels that can be employed in these devices. Thus, besides the commonly used fuels such as methanol and ethanol, efforts to identify alternative fuels for fuel cells are of great interest.

In this study, as an alternative to methanol, dimethoxymethane (DMM) and trimethoxymethane (TMM) are considered as alternative fuels, due to their similar energy density to methanol (DMM: 5.62 Ah g^{-1}, TMM: 5.05 Ah g^{-1} versus 5.02 Ah g^{-1} for methanol) and their availability as derivatives of natural gas [5–7]. The other reasons for the choice of these fuels are, these molecules do not contain any carbon–carbon bonds, i.e. fuels such as ethanol resists the complete electrooxidation to carbon dioxide due to carbon–carbon bond, and TMM has a higher boiling point, higher flash point, and lower toxicity compared to methanol [6]. Thus TMM and DMM may be promising alternative fuels for low-temperature fuel cells.

The majority of fuel cell anodes developed are based on gas diffusion electrodes and the structure of such electrodes typically comprise of a Nafion bonded catalyst layer and a gas diffusion layer, where the latter is made up of a microporous layer and Teflonised carbon cloth or carbon paper [8]. This structure is far from suitable for the transport and release of carbon dioxide gas from the anode, resulting potentially in considerably high hydrodynamic and mass transport limitations for liquid fuels at the anode [9,10]. Recently we have reported the use of titanium mini-mesh electrode coated with platinum-based catalysts as anode material for ethanol [11,12], formic acid [13] and ethylene glycol [14] fuel cells, which showed promising behavior in terms of gas removal characteristics and electrical performance in comparison to the conventional carbon supported membrane electrode assemblies. In this work, we investigate the electrooxidation of TMM and DMM on these mesh-based electrodes.

The complete electrooxidation of the TMM and DMM fuels could be described as follows. If hydrolysis of TMM or DMM preceded electrooxidation at the Nafion/electrode interface, the hydrolytic formation of methyl formate followed by

* Corresponding author. Tel.: +49 234 3222341; fax: +49 234 3214115.
E-mail address: raghu@techem.rub.de (R. Chetty).

0378-7753/$ – see front matter © 2007 Elsevier B.V. All rights reserved.
doi:10.1016/j.jpowsour.2007.07.068

formic acid would occur in the case of TMM, and formaldehyde would be produced in the case of DMM. Formic acid or formaldehyde (and methanol) could then be electrochemically converted to carbon dioxide [6,7,15]. These processes are shown below:

For TMM

$$(CH_3O)_3CH + H_2O \rightarrow HCO\text{–}OCH_3 + 2HCOH$$

$$HCO\text{–}OCH_3 + H_2O \rightarrow HCOOH + CH_3OH$$

$$HCOOH \rightarrow CO_2 + 2H^+ + 2e^-$$

For DMM

$$(CH_3O)_2CH_2 + H_2O \rightarrow 2CH_3OH + HCHO$$

$$HCHO + H_2O \rightarrow CO_2 + 4H^+ + 4e^-$$

Narayanan et al. [6] and Tsutsumi et al. [15] have reported that the performance of a fuel cell can be improved using TMM and DMM solutions instead of methanol and observed lower crossover rates than methanol.

This current paper describes an investigation of the electrooxidation of TMM and DMM at platinum-based binary catalyst, such as PtRu and PtSn, prepared by thermal decomposition on the titanium mesh, and the performances of these fuels in single direct liquid fuel cells were also evaluated.

2. Experimental

Titanium mesh (2Ti5-031, where strand width = 0.14 mm, thickness = 0.2 mm and ~1800 openings per square inch) was supplied by Dexmet Corporation, USA. $H_2PtCl_6{\cdot}6H_2O$, $RuCl_3{\cdot}xH_2O$ and $SnCl_2{\cdot}xH_2O$ were obtained from Alfa Aesar, dimethoxymethane, trimethoxymethane and sulfuric acid were receive from Aldrich.

2.1. Electrode preparation

Anodes were prepared by direct deposition of Pt-based catalyst on to the titanium mesh by thermal decomposition as described previously [10,11]. In brief, Ti substrates were dipped into 0.2 mol dm^{-3} chloride precursor solution in isopropanol and dried at 100 °C for 10 min, and this process repeated several times until the desired loading was achieved. The coated meshes were heat treated at 430 °C for 1 h. The electrodes prepared were sonicated with water and the amount of catalyst deposited was determined by comparing the substrate weight before and after deposition.

The atomic compositions of the electrodes were determined by energy dispersive X-ray analysis (EDAX), which was interfaced to a scanning electron microscope (Philips XL30 ESEM-FEG). The electrodes were further characterised by X-ray diffraction (XRD) using a Philips X'pert PRO diffractometer with Cu Kα radiation in the 2θ range from 20° to 90° scanning at a step of 0.02°. Diffraction peaks were attributed following the Joint Committee of Powder Diffraction Standards (JCPDS) cards. The catalyst compositions reported represent the average of three different measurements on the same sample measured by EDAX and these values represented a deviation <3%. The electrodes so prepared are denoted as PtRu/Ti (Pt:Ru = 1:1 in a/o) and PtSn/Ti (Pt:Sn = 1:1 a/o).

2.2. Electrochemical measurements

Cyclic voltammetry and chronoamperometry experiments were performed using a computer controlled PGZ100 Voltalab Radiometer potentiostat, loaded with VoltaMaster software. A conventional three-electrode system cell with a reference electrode connected with a Luggin capillary was employed for electrochemical measurements. The temperature of the cell was thermostated using a water circulator (Grant Ltd., Cambridge, UK). The working electrode was 1 cm^2 titanium mesh connected with a Ti wire with catalyst loading of 1 mg cm^{-2}. The counter-electrode was a platinum mesh and the reference electrode was a commercial mercury sulfate electrode (potential versus RHE is 0.65 V at room temperature). However, all the electrode potentials reported in this paper are referenced against the reversible hydrogen electrode (RHE). Experiments were conducted in 1.0 mol dm^{-3} DMM or TMM in 0.5 mol dm^{-3} H_2SO_4, purged with nitrogen.

2.3. Fuel cells

The single fuel cell used to assess the MEA performance consisted of two non-porous graphite blocks with a series of parallel channels machined into the block for the flow of fuel and oxygen. The active area of the anodes and cathodes was 2.25 cm^2 and the catalyst loadings of the anodes and cathodes were 3 mg cm^{-2}, respectively. Prior to data collection, the MEAs were fully hydrated by feeding Millipore water through the anode compartment at 60 °C for about 24 h. The 1.0 mol dm^{-3} DMM or TMM was flowed through the anode at a rate of 1 ml min^{-1}, and oxygen was passed to the cathode at a flow rate of 0.2 dm^3 min^{-1}. A Kenwood PEL-151 electronic load was used to obtain cell polarisation data.

2.4. MEA preparation

The catalyzed titanium mesh was used as anode, with 3 mg cm^{-2} metal loading. The cathode was a conventional electrode made from commercial 60 wt.% Pt/C (E-Tek) catalyst with Pt loading of 3 mg cm^{-2}, which consists of a backing layer, a gas diffusion layer and a catalyst layer. The backing layer consisted of carbon paper (Toray TGHP-090, E-Tek) to which a gas diffusion layer (GDL) was applied. The GDL consisted of ultrasonically mixed carbon black (Ketjen black 300), acetone and 10% PTFE suspension. Catalyst layers were then applied to the substrates by spraying an ultrasonically mixed ink containing the electrocatalyst, Nafion solution (Aldrich) and acetone. For comparison, conventional anodes were prepared using commercial (E-Tek) 20 wt.% PtRu/C or PtSn/C with 3 mg cm^{-2} metal loading. The electrodes were coated with 1 mg cm^{-2} of Nafion solution prior to forming a MEA. The membrane electrolyte used in this work was pre-treated Nafion 117. MEAs were prepared

by hot pressing the anode and cathode together with Nafion 117 membranes for 3 min at 130 °C and 100 kg cm^{-2}.

3. Results and discussion

3.1. X-ray diffraction

Fig. 1 shows the XRD patterns of various platinum-based catalysts prepared on titanium mesh substrate. The diffraction peaks around 39°, 46°, 68° and 81° are due to Pt (1 1 1), (2 0 0), (2 2 0) and (3 1 1) plane, respectively, which represents the typical character of a crystalline face centered cubic (fcc) phase of Pt. The (2 0 0) reflections of Pt are used to calculate the average particle size according to the Scherrer formula, and the particle mean size obtained from the XRD patterns were within the range of 90–100 nm. Due to the high solubility and smaller atomic size of ruthenium and tin, they are dissolved into the fcc structure of the platinum displacing the existing Pt atoms and do not therefore form their own hexagonal close packed lattice. The diffraction peaks of the binary alloy catalysts are shifted to lower 2θ values in the case of PtSn/Ti, and to higher 2θ values in case of PtRu/Ti with respect to the corresponding peaks in Pt/Ti.

3.2. Electrochemical characterisation

Cyclic voltammograms of thermally decomposed Pt/Ti, PtRu/Ti and PtSn/Ti scanned between the potentials of 0–1.2 V at the sweep rate of 20 mV s^{-1} and room temperature for DMM are shown in Fig. 2a. Fig. 2b shows the voltammogram of Pt/Ti in 0.5 mol dm^{-3} H_2SO_4 for a comparison, which shows the typical peaks for hydrogen/oxygen adsorption and desorption on the Pt surface. Fig. 2a for DMM oxidation presents the typical profile characterised by the inhibition of the hydrogen adsorption/desorption region, and the oxidation begins at potential greater than 0.40 V, with current density

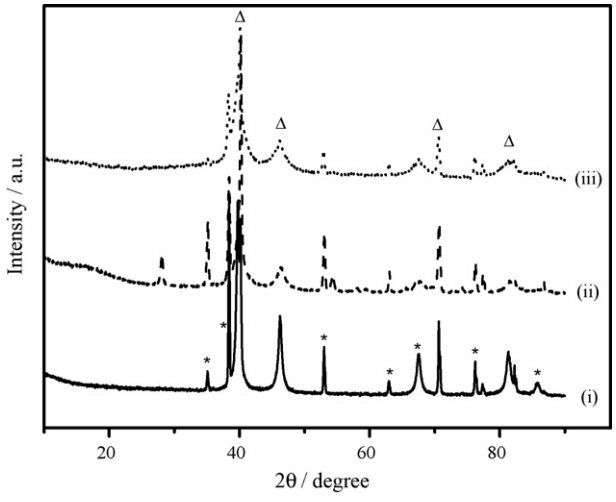

Fig. 1. X-ray diffraction patterns of thermally decomposed (i) Pt/Ti, (ii) PtRu/Ti and (iii) PtSn/Ti mesh substrates. Ti substrate is represented by * and △ represent diffractions of Pt.

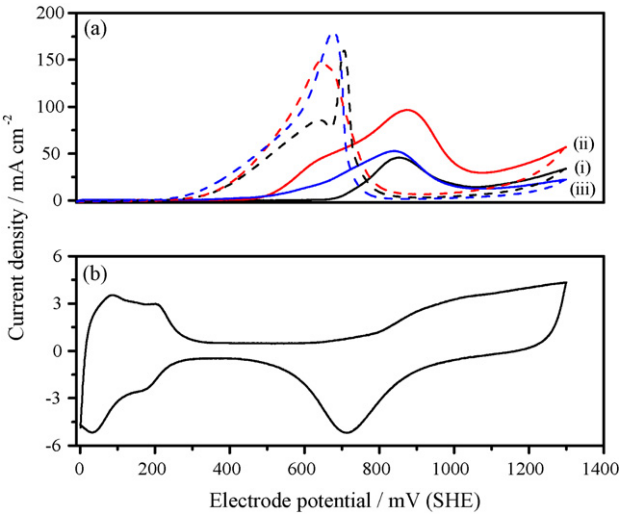

Fig. 2. (a) Cyclic voltammograms for the oxidation of 1 M dimethoxymethane in 0.5 mol dm^{-3} H_2SO_4 at 20 mV s^{-1} scan rate and room temperature on thermally decomposed (i) Pt//Ti, (ii) PtRu/Ti and (iii) PtSn/Ti electrodes. (b) Cyclic voltammogram of Pt/Ti in 0.5 mol dm^{-3} H_2SO_4.

peaks at 0.65 V and 0.88 V. The inhibition of the hydrogen adsorption/desorption peaks occurs due to the DMM adsorption in the potential <0.40 V. The anodic process is attributed to the oxidative removal of adsorbed/dehydrogenated DMM fragments (e.g. CO_{ads}) by PtOH species. During this process, CO, CO_2, HCOH, HCOOH and HCO–OCH_3 are formed and the CO molecule re-adsorbs, poisoning the catalyst surface [5,6,7,16]. This process is followed by a decline in the current density due to the formation of surface oxide. The increase in current density at potential >1.3 V can be associated with the oxidation of the species formed over the surface oxide. In the negative sweep, the voltammograms show a single oxidation peak, which is attributed to the oxidative decomposition of the by-products.

A detailed comparison of catalytic activity per milligram for TMM oxidation is presented in Fig. 3a, which show linear sweep voltammograms performed at a pseudo-steady state scan rate of 1 mV s^{-1}, in the potential range of 0–800 mV at 60 °C. Shown in Fig. 3b is a representative cyclic voltammogram for TMM oxidation at the PtRu/Ti electrode performed at a sweep rate of 20 mV s^{-1} and room temperature in the potential region of 0 V to 1.2 V. As evident from the shape of the voltammogram, it corresponds to that expected from the explanation of the oxidation of DMM, except for the value of the onset potential; where the reaction commenced at a potential around 0.50 V in comparison to 0.40 V for DMM and the current density peaks at a single potential of 0.90 V.

As can be seen in Figs. 2 and 3, enhancement in oxidation is observed with the addition of Ru and Sn in comparison with single Pt for the oxidation of both DMM and TMM. With the addition of Ru, the electrocatalytic activity is greatly enhanced, even at lower potentials. In the following section, the effect of operating parameters such as concentration of methoxy fuels and reaction temperature were studied on the mesh-based substrate coated with the PtRu catalyst.

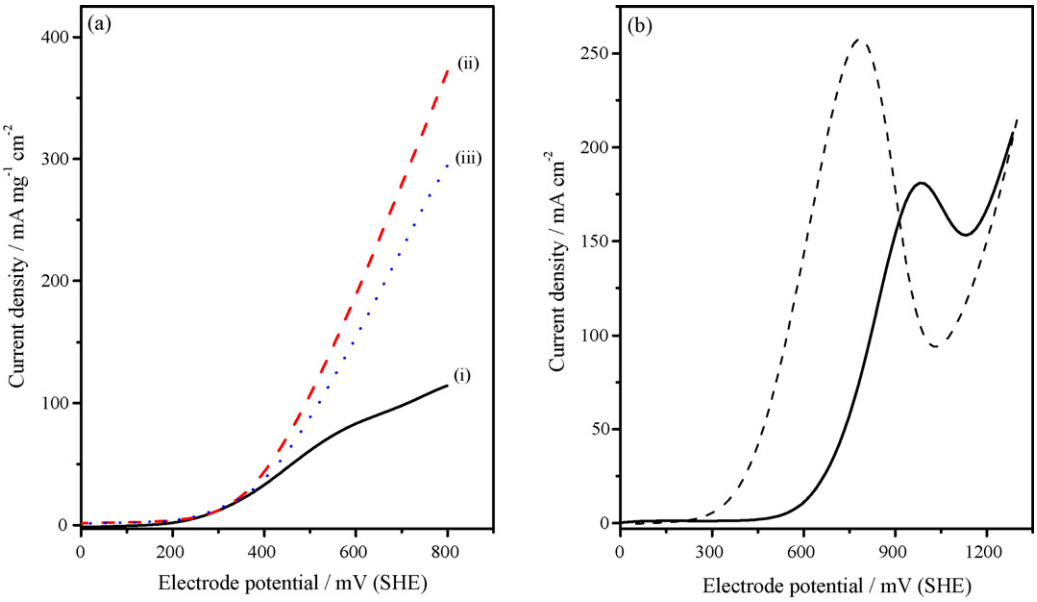

Fig. 3. (a) Linear sweep voltammograms for the oxidation of 1.0 mol dm^{-3} trimethoxymethane in 0.5 mol dm^{-3} H_2SO_4 at 1 mV s^{-1} scan rate and 60 °C on thermally decomposed (i) Pt//Ti, (ii) PtRu/Ti and (iii) PtSn/Ti electrodes. (b) Cyclic voltammogram of 1 mol dm^{-3} trimethoxymethane at PtRu/Ti electrode in 0.5 mol dm^{-3} H_2SO_4 at 20 mV s^{-1} scan rate and room temperature.

3.2.1. *Effect of trimethoxymethane concentration*

The effect of TMM concentration during the oxidation on the thermally decomposed PtRu/Ti electrode is shown in Fig. 4. Current–potential data were obtained in 0.5 mol dm^{-3} H_2SO_4 electrolyte, at a sweep rate of 1 mV s^{-1} and 60 °C with concentrations of 0.1 mol dm^{-3}, 0.5 mol dm^{-3}, 1.0 mol dm^{-3} and 2.0 mol dm^{-3} TMM. As can be seen from the figure, the oxidation current increased with increase in TMM concentration, up to 1.0 mol dm^{-3}, and a further increase in concentration resulted only in a slow increase in the current density. The effect of the DMM concentration on its oxidation at the PtRu/Ti electrode also resulted in similar performance, showing an increase in current density with increasing concentration. These observations agree well with the literature reported on DMM and TMM oxidation on carbon-based catalysts [6].

3.2.2. *Effect of reaction temperature*

Fig. 5 shows the effect of temperature on the oxidation of DMM at the thermally decomposed PtRu/Ti electrode. An oxidation current peak appeared at room temperature possibly due to the partial oxidation of DMM to the different by-products and/or dissociation to CO_{ads} intermediates. At higher temperatures, the oxidation became more facile and an increase in current density was observed on increasing the tempera-

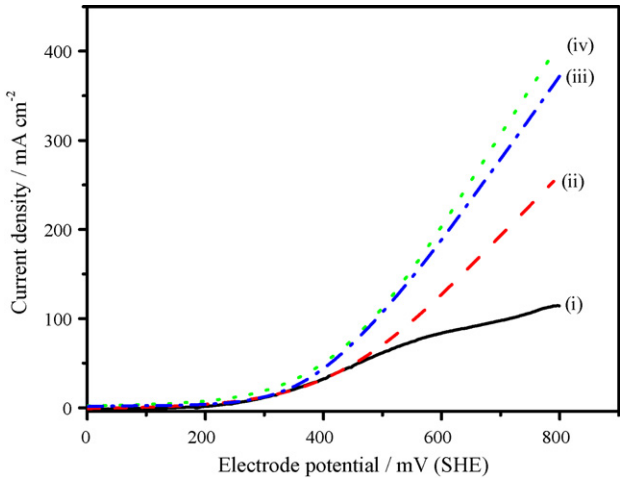

Fig. 4. Effect of TMM concentrations at thermally decomposed PtRu/Ti electrode in 0.5 mol dm^{-3} H_2SO_4 and 60 °C. Scan rate was 1 mV s^{-1}. (i) 0.1 mol dm^{-3}, (ii) 0.5 mol dm^{-3}, (iii) 1.0 mol dm^{-3} and (iv) 2.0 mol dm^{-3}.

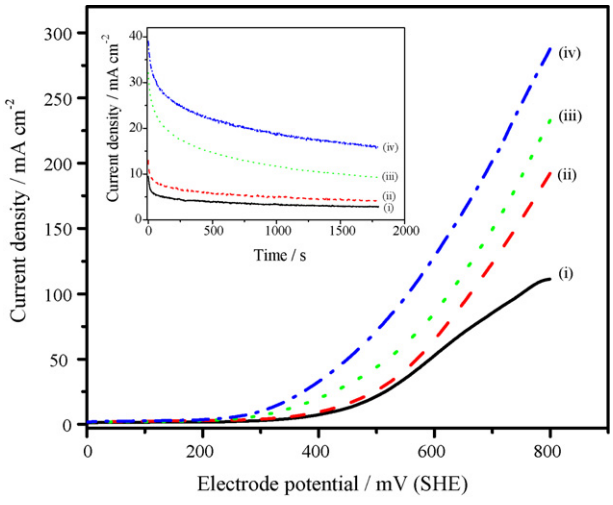

Fig. 5. Voltammograms for the oxidation of 1.0 mol dm^{-3} DMM in 0.5 mol dm^{-3} H_2SO_4 at 1 mV s^{-1} scan rate on thermally decomposed PtRu/Ti electrode as a function of temperature. Inset showing the chronoamperometric response recorded at 400 mV (SHE). (i) 21 ± 1 °C, room temperature (ii) 40 °C (iii) 60 °C and (iv) 80 °C.

ture from 21 ± 1 °C to 80 °C. These observations agree well with the literature [6], showing increased oxidation kinetics and less intermediate poisoning at higher temperatures. Fig. 5 inset shows the chronoamperograms obtained at 400 mV for the PtRu/Ti electrode at different temperatures. From the current–time profile, it is clear that the increase in temperature increases the current density, and the final current densities at 30 min were 15.9 mA cm^{-2} and 2.8 mA cm^{-2} for 80 °C and room temperature, respectively. The results are consistent with the linear sweep voltammogram results.

3.3. Fuel cell polarization

From the electrochemical characterisation presented above, it appears that the PtRu/Ti and PtSn/Ti catalysts showed higher catalytic activity than single Pt catalyst for both DMM and TMM oxidation. The catalytic activities of these electrocatalysts were then evaluated in a single direct fuel cell system.

Fig. 6 compares the polarisation curves of DMM for PtRu/Ti and PtSn/Ti mesh anodes employing Pt/C (E-Tek) cathode at 60 °C and 0.2 dm^3 min^{-1} oxygen. The open circuit voltage (OCV) observed is ca. 0.669 V for PtRu/Ti in comparison to 0.589 V observed for PtSn/Ti anode. A maximum power density of ca. 31 mW cm^{-2} was observed for the PtRu/Ti, while PtSn/Ti anode gave 26 mW cm^{-2}, which clearly indicates that the PtRu/Ti has high activity for DMM oxidation. As can be seen from the figure, in the low current density region, a larger cell voltage loss can be seen for the PtSn than with PtRu anode indicating a higher activation potential loss on the PtSn causing lower overall fuel cell performance. Peak power densities obtained with commercial PtRu/C and PtSn/C catalyst under similar operating conditions were 29.4 mW cm^{-2} and 26.6 mW cm^{-2} respectively, attained in the corresponding current density range of 100–130 mA cm^{-2}. From the observation presented above it is evident that PtRu/Ti is a better electrocatalyst for DMM oxidation in direct liquid fuel cells using Nafion membrane and agrees with the results obtained by the half-cell measurements.

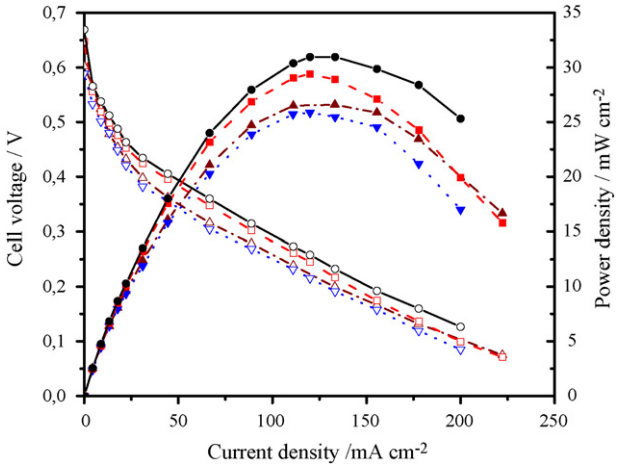

Fig. 6. Fuel cell polarisation data for thermally decomposed and commercial (E-TEK) catalysts measured at 60 °C in 1.0 mol dm^{-3} DMM and 0.2 dm^3 min^{-1} oxygen. Cathode catalyst: 3.0 mg cm^{-2}, 60 wt.% Pt/C (E-TEK) and anode catalyst loading 3 mg cm^{-2}. Current density (open symbol) and power density (blocked symbol) for: PtRu/Ti (◯, ●), PtRu/C (□, ■), PtSn/Ti (▽, ▼) and PtSn/C (△, ▲) anodes.

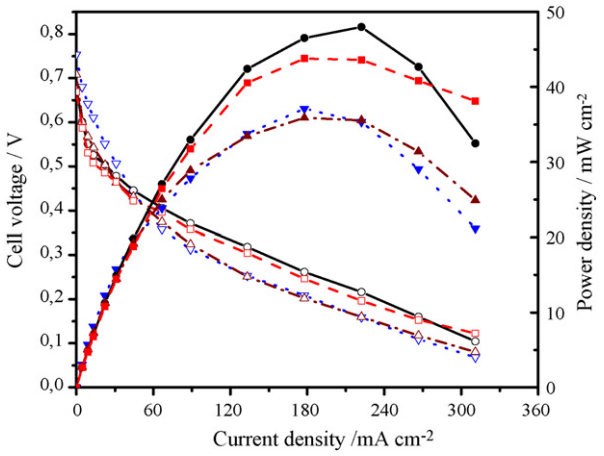

Fig. 7. Fuel cell polarisation data for thermally decomposed and (E-TEK) commercial catalysts measured at 60 °C in 1.0 mol dm^{-3} TMM and 0.2 L min^{-1} oxygen. Cathode catalyst: 3.0 mg cm^{-2}, 60 wt.% Pt/C (E-TEK) and anode catalyst loading 3 mg cm^{-2}. Current density (open symbol) and power density (blocked symbol) for PtRu/Ti (◯, ●), PtRu/C (□, ■), PtSn/Ti (▽, ▼) and PtSn/C (△, ▲) anodes.

Fig. 7 shows the voltage, power density and current density curves for 1.0 mol dm^{-3} TMM employing PtRu/Ti and PtSn/Ti mesh anodes and Pt/C (E-Tek) cathode at 60 °C and 0.2 L min^{-1} oxygen, from which it is clear that the power density with PtRu/Ti (48 mW cm^{-2}) is higher than that with PtSn/Ti (37.1 mW cm^{-2}). In the case of PtSn/Ti as anode, though the open circuit voltages are higher (0.754 V) than the corresponding values with PtRu/Ti (0.676 V) employed as the anode catalysts, it can be seen that there is a rapid initial fall in the cell voltage, whereas the voltage falls less with PtRu/Ti anodes in the low current density range. The rapid fall in the cell voltage could be caused by the slow oxidation reaction of TMM taking place on the surface of the PtSn electrode. This might suggest that the adsorbed species in the rate-determining steps for TMM and DMM oxidation could be different. The superior performance of the cell with TMM may also reflect the more facile oxidation of the intermediate formic acid formed, which does not occur with the oxidation of DMM. Peak power densities obtained with commercial PtRu/C and PtSn/C catalyst under similar conditions were 43.8 mW cm^{-2} and 35.9 mW cm^{-2} respectively. Wang et al. reported an open circuit voltage of 0.686 V and peak power density of ca. 60 mW cm^{-2}, obtained with TMM (TMM and water in a mole ratio of 1 to11.6) at 150 °C using phosphoric acid-doped polybenzimidazole membrane and PtRu (4 mg cm^{-2}) anode [7].

In order to examine the durability of the mesh-based electrodes, a short-term stability test was performed with the PtRu/Ti anode using 1.0 mol dm^{-3} TMM and oxygen at 60 °C. The result showed no significant difference in the fuel cell

performance even after running for 72 h, which indicates a relative stable cell performance achieved using the mesh-based anodes.

One factor that will need to be explored further with the use of these alternative fuels is the formation of by-products, and notably formaldehyde, and their subsequent presence or not in the spent fuel. It may be expected that formation of methanol will result in its subsequent oxidation. Interestingly the behaviour of methanol (1 mol dm^{-3}) in fuel cells gave power density of ca. 42 mW cm^{-2} under similar conditions to those used for TMM and DMM using the Ti-supported PtRu electrocatalyst. The performance achieved with the mesh electrodes has been with electrocatalysts with particle size much greater than that of carbon supported catalysts, thus there is potential for improvement in performance that could be gained in reducing the particle size. Moreover, the mesh-based electrodes offer many advantages in terms of simplicity, flexibility and ease of manufacture.

4. Conclusion

Electrooxidation of dimethoxymethane and trimethoxymethane has been demonstrated in acidic electrolytes on catalyst coated titanium mesh electrodes prepared by thermal decomposition of chloride precursors. PtRu and PtSn are efficient catalyst for the oxidation and the results suggest that DMM and TMM are promising alternative fuels for a fuel cell. The performance of the mesh-based anode was comparable to or even better than that with conventional carbon anodes. Direct liquid fuel cells employing the methoxy fuels can provide quite high power densities at near ambient conditions.

Acknowledgement

The authors would like to thank the United Kingdom Engineering and Physical Sciences Research Council (EPSRC) for the financial support.

References

[1] H.S. Liu, C.J. Song, L. Zhang, J.J. Zhang, H.J. Wang, D.P. Wilkinson, J. Power Sources 155 (2006) 95–110.
[2] K.M. McGrath, G.K.S. Prakash, G.A. Olah, J. Ind. Eng. Chem. 10 (2004) 1063–1080.
[3] S. Wasmus, A. Kuver, J. Electroanal. Chem. 461 (1999) 14–31.
[4] M.P. Hogarth, G.A. Hards, Platinum Met. Rev. 40 (1996) 150–159.
[5] N. Wakabayashi, K. Takeuchi, H. Uchid, M. Watanabe, J. Electrochem. Soc. 151 (2004) A1636–A1640.
[6] S.R. Narayanan, E. Vamos, S. Surampudi, H. Frank, G. Halpert, G.K.S. Prakash, M.C. Smart, R. Knieler, G.A. Olah, J. Kosek, C. Cropley, J. Electrochem. Soc. 144 (1997) 4195–4201.
[7] J.T. Wang, W.F. Lin, M. Weber, S. Wasmus, R.F. Savinell, Electrochim. Acta 43 (1998) 3821–3828.
[8] R.G. Allen, C. Lim, L.X. Yang, K. Scott, S. Roy, J. Power Sources 143 (2005) 142–149.
[9] C. Lim, K. Scott, R.G. Allen, S. Roy, J. Appl. Electrochem. 34 (2004) 929–933.
[10] L.X. Yang, R.G. Allen, K. Scott, P.A. Christenson, S. Roy, Electrochim. Acta 50 (2005) 1217–1223.
[11] R. Chetty, K. Scott, Electrochim. Acta 52 (2007) 4073–4081.
[12] R. Chetty, K. Scott, Fuel Cells (2007), submitted.
[13] R. Chetty, K. Scott, J. New Mat. Electrochem. Sys. 10 (2007) 135–142.
[14] R. Chetty, K. Scott, J. Applied Electrochem. 37 (2007) 1077–1084.
[15] Y. Tsutsumi, Y. Nakano, S. Kajitani, S. Yamasita, Electrochemistry (Tokyo Jpn.) 70 (2002) 984–987.
[16] A. Miki, S. Ye, T. Senzaki, M. Osawa, J. Electroanal. Chem. 563 (2004) 23–31.